

# Journal of the Arkansas Academy of Science

---

Volume 60

Article 5

---

2006

## Study of Causal Component Placement in an Active Sound Cancellation System

Eileen Anderson

*University of Arkansas at Little Rock, ebanderson@ualr.edu*

Andrew B. Wright

*University of Arkansas at Little Rock*

Follow this and additional works at: <http://scholarworks.uark.edu/jaas>

 Part of the [Other Physics Commons](#)

---

### Recommended Citation

Anderson, Eileen and Wright, Andrew B. (2006) "Study of Causal Component Placement in an Active Sound Cancellation System," *Journal of the Arkansas Academy of Science*: Vol. 60 , Article 5.

Available at: <http://scholarworks.uark.edu/jaas/vol60/iss1/5>

This article is available for use under the Creative Commons license: Attribution-NoDerivatives 4.0 International (CC BY-ND 4.0). Users are able to read, download, copy, print, distribute, search, link to the full texts of these articles, or use them for any other lawful purpose, without asking prior permission from the publisher or the author.

This Article is brought to you for free and open access by ScholarWorks@UARK. It has been accepted for inclusion in Journal of the Arkansas Academy of Science by an authorized editor of ScholarWorks@UARK. For more information, please contact [scholar@uark.edu](mailto:scholar@uark.edu).

# Study of Causal Component Placement in an Active Sound Cancellation System

EILEEN ANDERSON<sup>1,2</sup> AND ANDREW B. WRIGHT<sup>1</sup>

<sup>1</sup>Department of Applied Science, University of Arkansas at Little Rock, 2801 S. University, Little Rock, AR 72204

<sup>2</sup>Correspondence: ebanderson@ualr.edu

**Abstract.**—In a feedforward Active Sound Cancellation (ASC) system, the acoustic delay between a primary source and an error microphone must be greater than the delay between the measurement of that source by the reference microphone and the arrival of the secondary source's wave at the error microphone. Such a configuration is called a causal configuration. For periodic disturbances, cancellation can still be achieved in a non-causal configuration. Since the waveform is periodic, each cycle of the waveform is identical, and the cycle being canceled is not the measured part of the waveform, but a subsequent cycle in the waveform. Non-periodic sources cannot be cancelled by a non-causal ASC system, and convergence of the Least Mean Squares algorithm is not as effective in a non-causal configuration as in a causal configuration. The ASC system was implemented to create a local zone of silence inside a reverberant enclosure. The primary source was a 125 Hz sinusoid generated outside of the enclosure. System delays were calculated and a causal component configuration was chosen. System performance under both causal and non-causal component configurations was examined. The system was able to create a maximum attenuation of >18 dB in both the causal and non-causal configurations. However, it was discovered that in the non-causal configuration, the computation of the optimal inverse signal was much slower than in the causal configuration.

**Key words:**— Active Sound Cancellation (ASC), acoustic delay, waveform, Least Mean Squares algorithm.

## Introduction

Active Sound Cancellation (ASC), the attenuation of a sound field by constructive interference, has been proven to be a fertile area for research in recent years. A quiet space can be created in a noisy environment without foam, padding or acoustic tiles. ASC has been successfully tested in such diverse settings as mining vehicles (Stanef et al. 2004), high-rise apartments (Zhang et al. 2002), and MRI units (McJury et al. 1997). There are still many unanswered questions regarding the implementation of ASC, such as the ramifications of system causality.

In a feedforward ASC system, a reference microphone is placed where it can sense an unwanted acoustic noise, which is called the primary source. The microphone signal is sent to a controller. The controller computes an inverse signal and outputs it to a speaker located acoustically “downstream,” near an area where the sound is to be attenuated. This speaker is called the secondary source. Another microphone, called the error microphone, is placed where the zone of attenuation is desired (see Fig. 1).

The time required to measure the primary source, compute the inverse signal, broadcast the signal, and propagate the acoustic wave to the error microphone must be less than the time required for the primary source to propagate to the error microphone (Ffowcs Williams et al. 1985). Otherwise, the secondary source waveform will arrive after the primary source waveform has passed the error microphone. This constraint in active sound cancellation is called the causality constraint.

The constraint of causality has been acknowledged since ASC was first conceived. Lueg (1936) mentioned that active sound cancellation is dependent on the fact that “the speed of

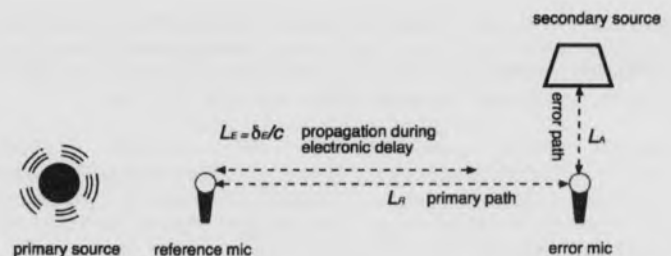


Fig. 1. Feedforward Active Sound Cancellation.

sound is very much less than the speed of electrical impulses” and that there should be ample time for activation of control elements within a circuit before the sound wave to be cancelled arrives. Ffowcs Williams et al, (1985) described the constraint of causality and discussed the causes of electronic delay. Nelson and Elliott (1992) presented a method for approximation of electronic delay based on the number of poles in the low-pass filters.

Several studies have demonstrated the effects of a causal configuration when canceling random noise. Tseng et al. (1998) moved the primary source in an arc while leaving the error and reference microphones stationary as the performance of an ASC system was recorded. When the primary source reached the bounds of a causal configuration, performance started to decline, and declined further as the configuration grew more non-causal.

## Study of Causal Component Placement in an Active Sound Cancellation System

Janocha and Liu (1998) showed in a simulation the deterioration in performance as increasing delay resulted in non-causality. Both of these studies presented results in terms of sound attenuation (dB) at the error microphone (real or simulated), but did not state the length of time that it took the system to reach the given attenuation.

Kong and Kuo (1999) used system efficiency as their metric. Efficiency reflects the percentage of the energy in the primary source that the ASC system is able to reduce. They showed theoretically and by simulation that the efficiency with which an ASC system cancels white noise decreases exponentially as a function of the degree of non-causality. Their simulation predicted that the system converges (albeit at different attenuation levels) in the same time whether the configuration is causal or non-causal.

Feedforward ASC can be performed with some success in a non-causal setting if the primary source is periodic and non-varying. Insufficient attention has been paid to causality, and many systems designed to cancel periodic noise are non-causal. Many researchers have claimed that causality is not important in such a system (Burdizzo et al. 1993, Kuo and Morgan 1996, Kang and Kim 1997, Bai et al. 2002). However, the effects of causality, when canceling periodic disturbances, have not been thoroughly investigated.

The work presented in this paper compares the performances of an ASC system canceling a periodic disturbance under both causal and non-causal conditions. A clear benefit of a causal ASC system for periodic disturbances will be demonstrated, and an "easy to use" test to determine whether a system is causal when it is set up will be suggested.

### Causality

Causal feedforward ASC depends upon the ability of the system to perform quickly enough to output the secondary source before the primary source's sound wave has propagated to the error microphone. While the sound waves generated by the primary source are travelling to the error microphone, the following events must take place:

1. The reference microphone must sense the sound from the primary source.
2. The reference microphone's signal must travel through the electronic filters and arrive at the controller.
3. The controller must compute the value of the primary source at the error microphone, using the reference microphone signal and the error microphone signal.
4. The controller must compute and output the secondary source signal.
5. This signal must travel through the electronic filters and arrive at the secondary source.
6. The sound must travel from the secondary source to the error microphone.

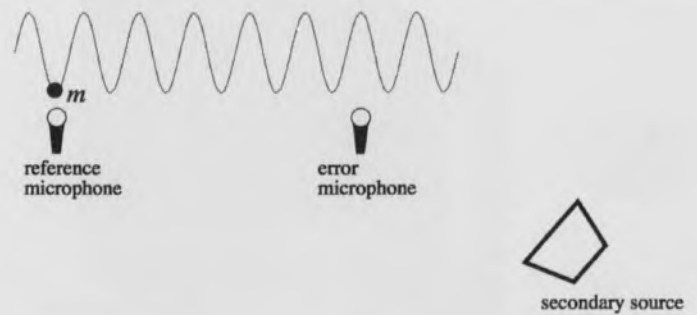


Fig. 2a. Element of acoustic wave at time  $t_0$ .

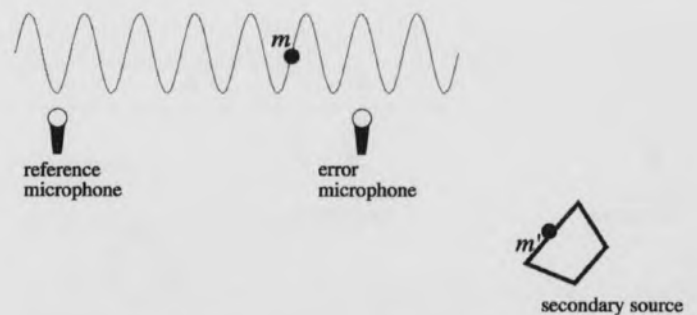


Fig. 2b. Element of acoustic wave at time  $t_0 + \delta_E$ .

Each of these events takes time. The combined times for the first 5 items comprise the electronic delay,  $\delta_E$ . Let the time of the sixth item be  $\delta_A$  and the time necessary for the primary source to propagate acoustically from the reference microphone to the error microphone be  $\delta_R$ .

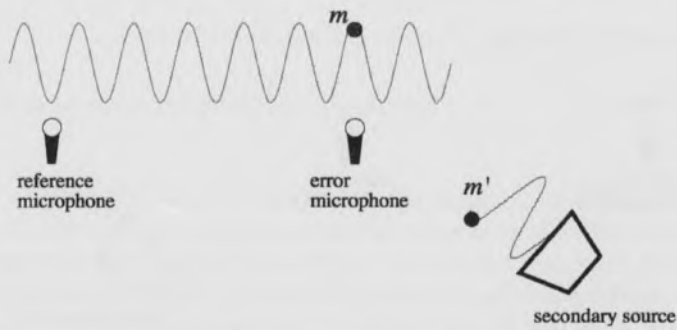
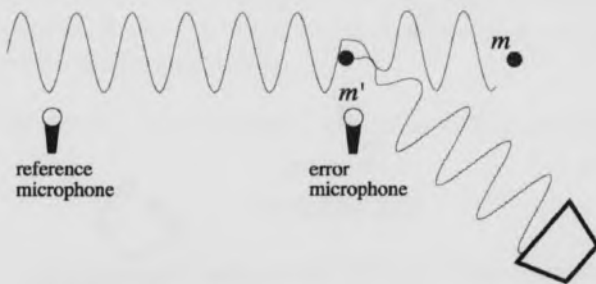
Both  $\delta_A$  and  $\delta_R$  are acoustic delays, and the lengths of the respective acoustic paths are  $L_A/c$  and  $L_R/c$ , where  $c$  is the speed of sound (see Fig. 1). To fulfill the constraint of causality,

$$\delta_R - \delta_A \geq \delta_E. \quad (1)$$

For a causal configuration, the components must be arranged such that their respective distances and the electronic delay allow Equation 1 to be satisfied.

Periodic noise can be cancelled by a non-causal system. Consider an element,  $m$ , of an acoustic wave propagating from the reference microphone to the error microphone.

The reference microphone senses an acoustic wave at time  $t_0$  (see Fig. 2a). When the electronic delay has ended at  $t_0 + \delta_E$ , the wave has propagated through a distance  $c(t_0 + \delta_E)$  as shown in Fig. 2b. The controller has finished calculating the inverse wave, and the output signal has reached the secondary source. The inverse wave, with element  $m'$  similarly marked, begins to travel. The primary source arrives at the error microphone at  $t_0$

Fig. 2c. Element of acoustic wave at time  $= t_0 + \delta_R$ Fig. 2d. Cancellation occurring in non-causal configuration at time  $= t_0 + \delta_E + \delta_A$ 

$+ \delta_R$  (see Fig. 2c). In this example, the electronic delay was too long, and the point  $m'$  on the inverse signal that was computed to cancel  $m$  didn't reach the error microphone in time.

However, at  $t_0 + \delta_E + \delta_A$  (see Fig. 2d), when the wave from the secondary source reaches the error microphone, the phase of the primary source will approximate its value at  $t_0 + \delta_R$ . If the difference is only a few cycles, the controller can make the necessary adjustments to cancel the sound at the error microphone.

The secondary source output was calculated to cancel the sound one or more cycles previous to the cycle actually present at the error microphone. The sound is still canceled but only because of the periodicity, not because the system can predict the sound present at the error microphone.

A non-causal system synchronizes the secondary source phase with the primary source waveform at the error microphone modulo  $2\pi$ , if the primary source waveform is sinusoidal. If the primary source waveform is not truly sinusoidal, such synchronization cannot occur. This situation arises in random signals and non-periodic signals, such as speech.

Should a non-causal system be applied to cancel a non-periodic disturbance, the cancellation would not occur. Since real world acoustic disturbances are rarely completely static, a

non-causal system is not reliable.

## Materials and Methods

**ASC System.**—The causality experiments were conducted using the ASC system at the University of Arkansas at Little Rock (UALR). The system uses an Integrated Motions, Inc. MX31 embedded controller with preamplifiers and anti-aliasing filters to condition the signals from the microphones and anti-imaging filters to condition the signals to the speakers (see Fig. 3).

The ASC algorithm was designed in block diagram form using Simulink software and converted into C code using Real-Time Workshop. The controller sample rate was 1000 Hz. Both the primary and secondary sources were generated by JBL J520M speakers with a flat frequency response from 70 Hz to 20 kHz. An ADCOM GFA-6000 five-channel 100 Watt-per-channel audio power amplifier powered the speakers.

The frequency of the primary source was chosen as 125 Hz. A Galois test signal was added to the output of the secondary source to improve system identification. The test signal was composed of 127 harmonics from 3.906 to 500 Hz (Xie 1997). The frequency components of the Galois signal actually generated ranged from approximately 70 Hz to 500 Hz because of the lower limit of the speaker.

Custom circuits were used to condition the signals. Two microphone preamplifier circuits amplified the low-level microphone output signal and limited the radio frequency noise in the system. Two amplifier-filter circuits further amplified the microphone signals to occupy the range of the  $\pm 10$  V ADC channels in the MX31 controller, and implemented a low-pass anti-aliasing filter. Two attenuator circuits reduced the output of the MX31 to the  $\pm 5$  V input range of the power amplifier and also implemented a low-pass anti-imaging filter. The low-pass filters had a cut-off frequency of 693 Hz.

The error and reference microphones were both Radio Shack

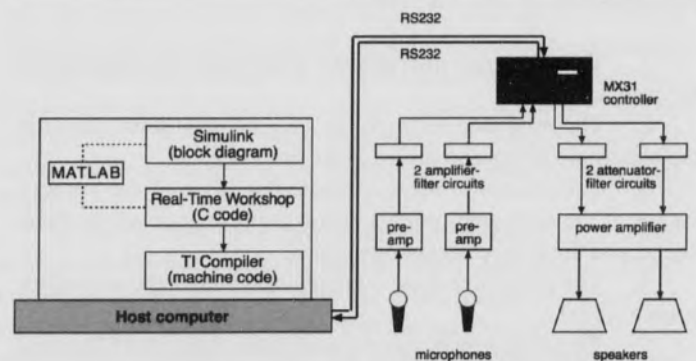


Fig. 3. Experimental hardware.



Study of Causal Component Placement in an Active Sound Cancellation System

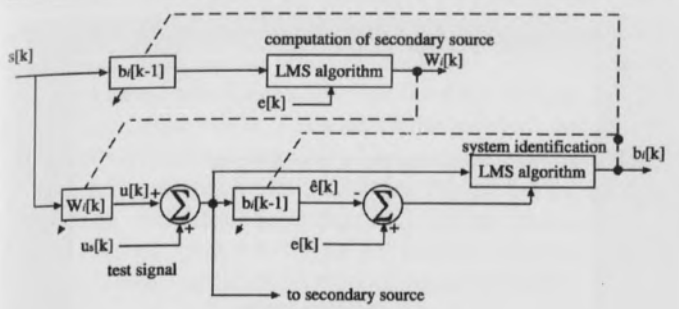


Fig. 4. Controller structure.

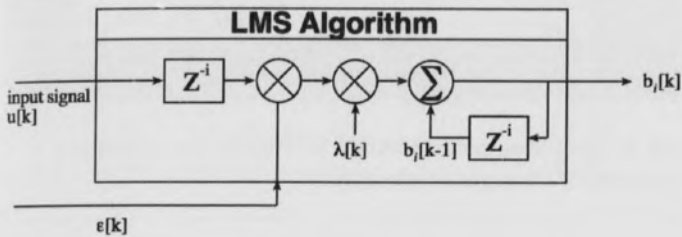


Fig. 5. Block diagram of least mean square algorithm.

No. 270-090 condenser type microphones with a flat frequency response from 20 Hz - 20 kHz.

**Algorithm.**—The controller performed two adaptive processes: system identification and computation of the filter coefficients used to generate the secondary source (see Fig. 4). The normalized Least Mean Square (LMS) algorithm was used in both of these processes (Fig. 5). It uses a gradient descent mechanism with a convergence parameter  $\lambda[k]$  to minimize an error,  $\epsilon[k]$ . The convergence parameter  $\lambda[k]$  is adaptive (Goodwin and Sin 1984), modified by the magnitude of the filter coefficients,  $b_i$ :

$$\lambda = \mu \left( \sum_{i=1}^{N_b} b_i^2 \right)^{-1}, \quad (2)$$

where  $N_b$  is the length of the filter and  $\mu$  is a fixed convergence parameter.

In the system identification process, a finite impulse response (FIR) filter generates an estimate,  $\hat{e}[k]$ , of the error signal  $e[k]$  sensed by the error microphone:

$$\hat{e}[k] = \sum_{i=0}^{N-1} b_i[k]u[k-i], \quad (3)$$

where  $N$  is the number of filter coefficients and  $u[k]$  is the generated control signal. The algorithm to update the  $N$

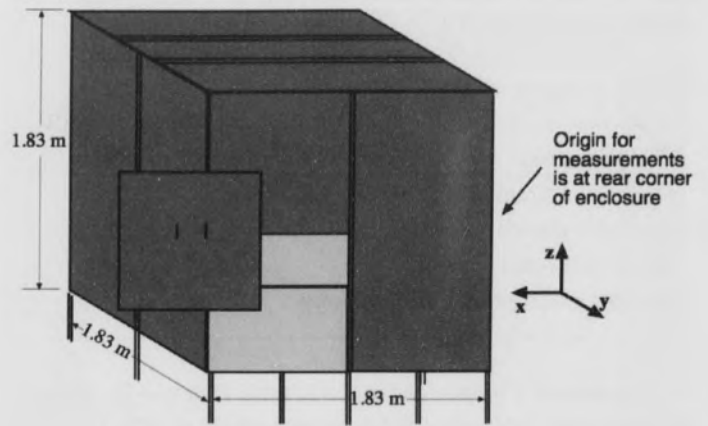


Fig. 6. Acoustic enclosure.

coefficients is

$$b_i[k] = b_i[k-1] + \lambda \epsilon \mu [k-1]. \quad (4)$$

In the controller's computation of the filter coefficients to generate the secondary source, the LMS algorithm minimizes the signal  $e[k]$  from the error microphone.

**Enclosure.**—The experiments were performed in UALR's acoustic enclosure. It is constructed of Unistrut™ steel framing and 1/4-inch exterior grade plywood (see Fig. 6). The floor of the structure is elevated with a clearance of 0.305 m to prevent coupling with the room floor.

The enclosure's internal dimensions are 1.83 m x 1.83 m x 1.83 m. The enclosure has no soundproofing, so external sounds are admitted. Extraneous sounds during the experiments were mainly low frequencies generated by the building ventilation system.

The first set of normal modes of the enclosure occurs at 94 Hz and the Schroeder frequency is approximately 400 Hz. The 125-Hz primary source generated a reverberant but non-diffuse sound field in the enclosure.

Computation of Causal Configuration

To establish a causal system, it was necessary to measure the delay of all system components. The components of the ASC system were tested, separately and in combination, for delays so that the total delay of the system could be known (Anderson 2004). The acoustic delays were known from the distance of the reference microphone to the error microphone and the speed of sound.

**Component Delays.**—The system components were tested with square waves at several frequencies and several sample

times. A 125-Hz square wave sampled at 1 kHz yielded the results shown in Table 1.

Table 1. Component Delays

Component(s)	Delay
Attenuator circuit	2 ms
Amplifier circuit	2 ms
MX31 controller	1 ms
Speaker, microphone, and pre-amp	2 ms

**Combined Component and Acoustic Delay.**—To measure the combined component delay, square waves at 100, 125, 200, and 250 Hz were generated in a Simulink model, output through a DAC block to the MX31, and output from the MX31 to the attenuator circuit. The signal from the attenuator circuit was fed to the power amplifier, which generated an output to the speaker. The acoustic waves propagated 15 cm to the microphone. The microphone signal was fed to the pre-amplifier, then to the amplifier circuit. The output of the amplifier circuit was connected to the MX31, then fed to the workspace through an A/D block (see Fig. 7).

The combined delay at 125 Hz sampled at 1 kHz was approximately 8 ms. This result agrees well with the sum of the delays of the separate components. The 8 ms delay included an acoustic propagation time of 43 ms, low enough to be ignored when computing the electronic delay alone. The uncertainty due to component placement was about 15 ms for each component, also low enough to be ignored. However, there was an uncertainty of half of the sampling time in the delay. Therefore, the value of the electronic delay used for calculating component placement was  $8 \pm 0.5$  ms.

**Placement of Microphones and Secondary Source.**—The primary source speaker was placed outside of the enclosure. This placement emulated the common real-world situation of break-in noise, wherein an unpleasant external noise source enters a vehicle, control room, or other enclosed area intended for human use.

Possible placements of components to achieve a causal system, given the location of the primary source, were calculated

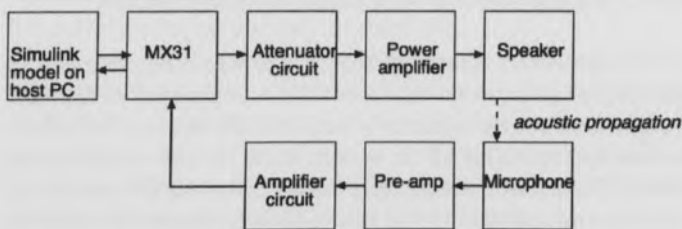


Fig. 7. Combined delay testing set-up.

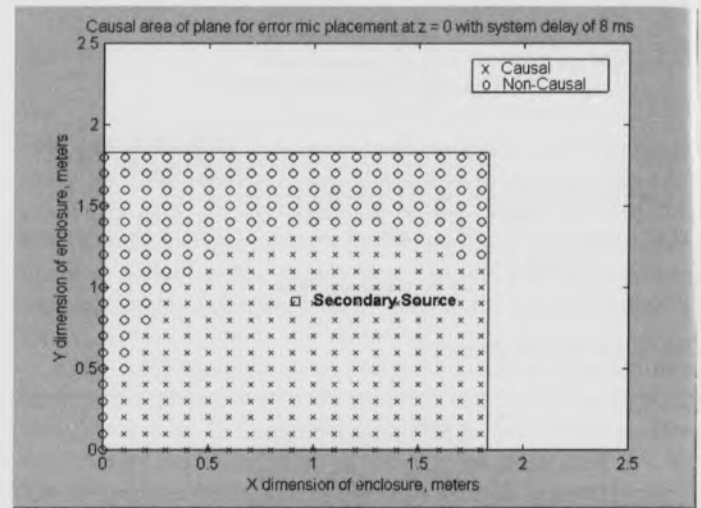


Fig. 8. Sample output of MATLAB program for computing causal error microphone placement.

using a custom MATLAB program. The program used Equation 1 to check the causality at discrete points on a horizontal plane in the enclosure (see Fig. 8).

The reference microphone was placed 10 cm from the primary source. Causal placements for the error microphone and secondary source on the floor of the enclosure were chosen from possible values shown by the program (see Table 2).

Table 2. Location of ASC components

Component	Location (m)
Primary source location	(0.03, 3.28, 2.52)
Reference microphone location	(0.02, 3.18, 2.52)
Secondary source location	(0.91, 0.91, 0.23)
Error microphone location	(1.25, 0.66, 0.22)

The minimum acoustic delay necessary between the reference microphone and error microphone to fulfill the constraint of causality in the chosen configuration was computed. The minimum delay was a sum of the electronic delay,  $\delta_E$  and the propagation time from the secondary source to the error microphone,  $\delta_A$ . With  $\delta_E = 8 \pm 0.5$  ms and  $\delta_A = 1.2$  ms, the necessary delay was  $\geq 9.2 \pm 0.5$  ms. The component placements in Table 2 fulfill causality with  $\delta_R = 10.5$  ms.

## Experiments

ASC was performed with the components in the chosen causal configuration. System identification was performed for 35 seconds with the Galois noise power level set at 0.1. This

## Study of Causal Component Placement in an Active Sound Cancellation System

level was chosen after testing the coherence between the Galois test signal and the error microphone (Wright and Craig 1998). System identification and the computation of the inverse signal were performed simultaneously with the filter weights reset to zero for each experiment. The sound from the error microphone and the behavior of the algorithm filter weights were recorded.

The reference microphone was then moved toward the error microphone such that the distance  $L_R$  and the delay  $\delta_R$  grew shorter. ASC was performed again and the same parameters were recorded. Table 3 summarizes the experimental results.

Table 3. Results of Causality Experiments

Exp	$L_R$ (m)	$\delta_R$ (ms)	Attenuation in 35 seconds
1	3.61	10.5 (causal)	18.4 dB
2	3.19	9.3 (near causal threshold)	17.2 dB
3	3.08	9.0 (non-causal)	6.1 dB
4	2.90	8.4 (non-causal)	0 dB

The computation of the electronic delay predicted a threshold for a causal configuration between 8.7 and 9.7 ms. The  $\delta_R$  value of 9.3 ms in Experiment 2 is near that threshold. In that experiment, the error signal attenuation settled to slightly less than the value for the causal configuration within 35 seconds. Experiment 3, with a  $\delta_R$  value of 9.0 ms, had much slower attenuation. The convergence of the control algorithm was so slow during the other experiments that no attenuation was achieved in the first 35 seconds.

Other experiments with convergence times of several minutes showed that the maximum attenuation reached in the causal configuration could eventually be reached in the non-causal configurations. This effect is not mentioned in the studies using random noise (Tseng et al. 1998, Janocha and Liu 1998) and is probably not possible with random noise.

The system identification filter convergence time was unaffected by causality, as predicted by Kong and Kuo (1999). However, the convergence of the control filter taps appeared to be affected by causality, with convergence occurring more slowly in the non-causal configurations.

Fig. 9 shows the attenuation at the frequency of the primary source over 35 seconds for Experiments 1 (causal) and 3 (non-causal). FFTs were performed for each second of error microphone data to isolate the primary source frequency from the Galois noise (recall that the calculation of the inverse signal and system identification are performed simultaneously). The increase in sound pressure level (SPL) at the beginning of the causal plot is caused by the secondary source. Its output briefly increases the SPL at the error microphone before the optimal inverse wave is computed. The brief but audible increase in SPL proved to be present whenever ASC was performed in a causal configuration and served as a convenient indicator of a

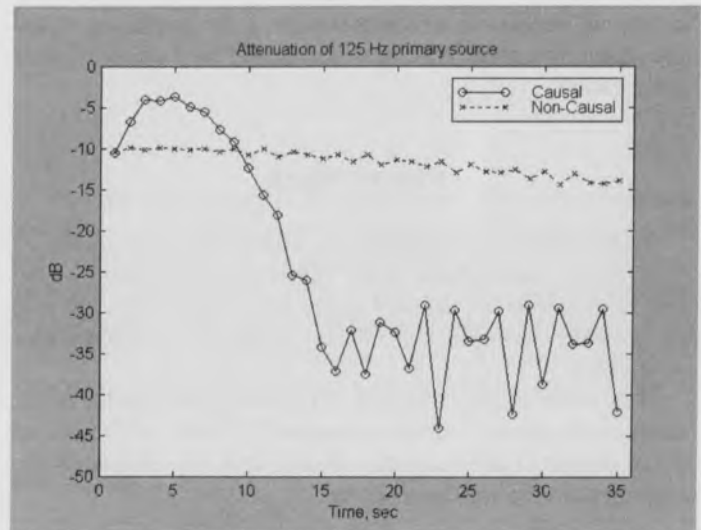


Fig. 9. Attenuation of 125 Hz primary source in causal and non-causal configurations.

configuration's causality.

The attenuation of the sound at the error microphone was much faster in the causal experiment and reached steady state in about 15 seconds. In the near-causal experiment, attenuation was nearly complete at 35 seconds. During the non-causal experiments, it took several minutes. This demonstrates that the computation time for the inverse signal in the non-causal system is much too long to be practical in most real-world applications. Since an ASC system must adapt to environmental changes, the very slow non-causal response may lead to poor performance or instability.

## Conclusions

An ASC system was implemented to cancel a periodic disturbance in an enclosure. After computing causal positions for the components, and testing the system in that configuration, the reference microphone was moved into non-causal positions. The performance of the system in the non-causal configurations with increasing delays was recorded. Three potential contributions to knowledge are suggested by the results. First, a clear benefit of a causal ASC system for periodic disturbances was demonstrated: the much greater speed of computation of the inverse signal. This is contrary to previous comments about the irrelevance of causality when canceling periodic disturbances. Second, this study may be the first to verify, through experiment, the role of causality in the speed of algorithm convergence. The system identification filter convergence time was unaffected by causality, as predicted by Kong and Kuo (1999). However, the convergence of the control filter was affected by causality. Finally, a mark of



system causality was found that may be previously unreported. An audible increase in SPL was present at the beginning of the experiment whenever ASC was performed in a clearly causal configuration.

### Future Work

Experiments implementing an added electronic delay of the reference microphone signal rather than movement of the error microphone are already under way. They will eliminate any possible environmental effects caused by the microphone movements.

The cause of the increased SPL before convergence in the causal configuration will be determined. A limit will be placed on the output of the secondary source and any effects on the convergence time will be observed.

### Literature Cited

- Anderson EB.** 2004. Characterization of active sound cancellation zone of silence in reverberant enclosure with periodic disturbance [MS thesis]. Little Rock (AR): University of Arkansas at Little Rock. 160 p.
- Bai MR, Y Lin, and J Lai.** 2002. Reduction of electronic delay in active noise control systems—a multirate signal processing approach. *Journal of the Acoustical Society of America* 111:916-24.
- Burdisso RA, JS Viperman, and CR Fuller.** 1993. Causality analysis of feedforward-controlled systems with broadband inputs. *Journal of the Acoustical Society of America* 94:234-42.
- Ffowcs-Williams JE, I Roebuck, and CF Ross.** 1985. Anti-phase noise reduction. *Physics Technology* 16:19-24.
- Goodwin GC and KS Sin.** 1984. Adaptive filtering, prediction, and control. Prentice-Hall, Englewood Cliffs, NJ. 540 p.
- Janocha H and B Liu.** 1998. Simulation approach and causality evaluation for an active noise control system. *IEE Proceedings Control Theory and Applications* 145:423-6.
- Kang SW and YH Kim.** 1997. Causally constrained active sound power control in an enclosed space. *Journal of Sound and Vibration* 204:807-22.
- Kong X and SM Kuo.** 1999. Study of causality constraint on feedforward active noise control systems. *IEEE Transactions on Circuits and Systems II—Analog and Digital Signal Processing*:64:183-6.
- Kuo SM and DR Morgan.** 1996. Active noise control systems. New York: Wiley. Appendix B, Practical System Considerations; p 323-34.
- Lueg P** (inventor and assignee). 1936. Process of silencing sound oscillations. US Patent 2,043,416.
- McJury M, RW Stewart, D Crawford, and E Toma.** 1997. The use of active noise control (ANC) to reduce acoustic noise generated during MRI scanning; some initial results. *Magnetic Resonance Imaging* 15:319-22.
- Nelson PA and SJ Elliott.** 1992. Active control of sound. San Diego, CA: Academic Press. Chapter 6, Single channel feedforward control; p 161-203.
- Stanef DA, CH Hansen, and RC Morgans.** 2004. Active control analysis of mining vehicle cabin noise using finite element modeling. *Journal of Sound and Vibration* 277:277-97.
- Tseng W, B Rafaely, and SJ Elliott.** 1998. Combined feedback-feedforward active control of sound in a room. *Journal of the Acoustical Society of America* 104:3417-25.
- Xie B.** 1997. A comparison of test signals used in active sound cancellation [MS thesis]. Little Rock (AR): University of Arkansas at Little Rock. 87 p.
- Wright AB and KC Craig.** 1998. Use of Schroeder phased waveform to investigate convergence and tracking of the LMS algorithm in active sound control. *Applied Acoustics* 53:95-116.
- Zhang J, W Jiang, and N Li.** 2002. Theoretical and experimental investigations on coherence of traffic noise transmission through an open window into a rectangular room in high-rise buildings. *Journal of the Acoustical Society of America* 112:1482-95.